Korean J. Chem. Eng., 39(1), 134-145 (2022)
DOI: 10.1007/s11814-021-0970-6

pISSN: 0256-1115
eISSN: 1975-7220

Extraction of dysprosium from waste neodymium magnet solution with ionic liquids and ultrasound irradiation procedure

Mehdi Asadollahzadeh† **and Rezvan Torkaman**†

Nuclear Fuel Cycle Research School, Nuclear Science and Technology Research Institute, P.O. Box: 11365-8486, Tehran, Iran

(*Received 18 March 2021 • Revised 26 September 2021 • Accepted 29 September 2021*)

Abstract−This study investigated imidazolium ionic liquids' capability under ultrasonic irradiation conditions for dysprosium extraction from the aqueous nitrate solution. The main objective was to evaluate the feasibility of ultrasound-assisted extraction techniques compared to conventional solvent extraction. The extraction process was investigated as a function of the ionic liquids and organic extractant, organic/aqueous phase volume ratio, the acidity of the aqueous phase, contact time, ion concentration, temperature, and stripping condition. The outcomes demonstrated that the combination of $C_6MIM.PF_6$ and TOPO extractant is more extractable than the mixture of $C_6MIM.NTf_2$ and TOPO. The effects of ultrasonic irradiation on the Dy(III) ions show that ion transfer occurs with high extraction efficiency. The variation of logD versus temperature demonstrated that temperature had little impact on the extraction procedure. The recovery of dysprosium ions from the organic phase using 0.5 M nitric acid is achieved in stripping studies. The results showed that the extraction and recovery under ultrasonic irradiation and with the presence of ionic liquids proposed a simple and environmentally friendly approach for the purification and separation of rare-earth ions from the permanent magnet wastewater.

Keywords: Imidazolium Ionic Liquid, Ultrasonic Irradiation, Rare Earth Ions, Permanent Magnet Wastewater

INTRODUCTION

One of the largest dysprosium industries globally is involved in creating permanent magnets [1]. The resistivity in high temperature is one reason for the utilization of (Nd, Dy)-Fe-B magnets in engines and generators [2,3]. The demand for dysprosium ions is rapidly increasing due to the particular application of magnets [4]. Dysprosium is one of the rare earth metals extracted by various processes from the rare earth minerals, such as basic and acidic leaching, solvent extraction, and ion exchange [5]. In addition to the original production process, recovery procedures have been developed to bring this strategic metal back to industry [6,7]. Wastewater management is essential in all processes, and the improvement of methodologies is one of the most critical needs due to the reduction of environmental impacts [8]. Green chemistry has been introduced in recent years to develop modern processes and eliminate environmental pollution [9].

Green solvents are an essential stage in improving new procedures, and research works into the applicability of ionic liquids have increased in the literature [10-17]. Sun and co-workers showed the association of saponification technique and ionic liquid in separating different rare earth elements. The separation process of lanthanum from yttrium was reported during two extraction stages and four washing stages [18]. Application of triphosphine trioxide ligand in two ionic liquids ($[EBPip][NTf_2]$, and $[EOPip][NTf_2]$) showed that the obtained mixture for the separation of rare earth elements had higher efficiency than the dibenzyl ether solvent [19]. Young and co-workers synthesized a new ionic liquid for the extraction and precipitation of rare-earth elements. The synthesized sample was applied to recover praseodymium from the Nd-Fe-B magnet wastewater, and 99.85% recovery was obtained after the iron removal stage [20]. The separation of scandium was investigated by using $[C_nMIM.NTf_2]$ as an ionic liquid and carboxyl-functionalized ionic liquids as an extractant. The outcomes showed that 99.5% of the scandium ions could be separated from the mixture of lanthanides with a high separation factor (~1,000) [21]. Recovery of Dy(III) and Nd(III) from permanent magnets was studied with ionic liquid (trihexyl(tetradecyl)phosphonium chloride) and EDTA as a complexing reagent. The oxide compounds of the Dy(III) and Nd(III) were prepared with high purity of 99.6%, and 99.8%, respectively. The results confirmed that ionic liquids could be utilized in the recovery process with high efficiency [22]. Chen and co-workers investigated the effect of [A336][P507] as a bifunctional ionic liquid extractant for the solvent extraction of heavy rare earth elements. The proton-exchange mechanism in the ionic concentration of less than three mol/L, ion-pair mechanism above seven mol/L, both in the range 3-7, were reported with this extractant [23].

Extraction of dysprosium ions with organic solvents such as PC88A [24], D2EHPA [24], Cyanex923 [25], Cyanex572 [26], and Cyanex272 [27] was investigated in the literature. The outcomes showed that different parameters such as temperature, time, the concentration of salts, and extractants influenced the extraction efficiency. Also, mixing is significant in the extraction process; for this reason, various agitated columns have been used to extract rare earth metals [28-35]. The use of ultrasonic waves is one of the suitable

---

†To whom correspondence should be addressed.
E-mail: masadollahzadeh@aeoi.org.ir, mehdiasadollahzadeh@iust.ac.ir,
mehdiasadollahzadeh@yahoo.com, rtorkaman@aeoi.org.ir

alternatives to the mechanical mixing process. The enhancement in the ion transfer rate between two phases is provided by the waves and the formation of microbubbles [36]. The increase in mass transfer rates and slight variations were reported in hydrodynamic parameters under ultrasonic waves [37]. Daryabor and co-workers investigated the potential of ultrasonic waves to extract zinc and cadmium ions from sulfate media. The result showed that cadmium ions were affected by the ultrasonic waves, and their transfer rate decreased to the organic phase. However, these waves did not impact the extraction efficiency of zinc ions [38]. The ultrasonic process has particular advantages, such as reducing the stagnant regions between two phases and enhancing circulation. Most studies have been investigated in the solid-liquid phase systems [39-43]. Also, few studies have been performed on extracting rare earth metal dysprosium by using ionic liquids. This study investigated the dysprosium extraction from aqueous solution under ultrasound-assisted extraction technique with ionic liquids. Also, the mechanical mixing system and the utilization of commercial organic solvents were studied to compare and describe the procedure. The effects of main parameters on the extraction efficiency were investigated, and the ion transport mechanism was reported by the relationship between distribution ratio and the variation of main parameters. The application of ultrasonic and mechanical mixing conditions showed that dysprosium ions could be extracted using these procedures and the imidazolium ions.

EXPERIMENTAL

1. Chemical Materials

For experimental work, trioctylphosphine oxide purchased from the Aldrich company was utilized as the organic extractant. Imidazolium ionic liquid ($C_6MIM.NTf_2$ and $C_6MIM.PF_6$) as an extractant and a diluent was purchased from synthesized samples in the Iranian Petroleum Research Institute. Kerosene was used as a diluent in the comparative study with ionic liquid. The feed solution was prepared by dissolving the dysprosium nitrate hexahydrate, 99.9% (the Middle East Alloy company) in deionized water. The recovery solution in the stripping phase was prepared by using a nitric acid solution with a specific concentration.

2. Extraction Procedure

The extraction process was performed by selecting 5 mL from two aqueous and organic phases and their contact. The aqueous phase was prepared with a specific concentration of dysprosium (250 ppm) in nitric acid medium, and the organic solvent was prepared from ionic liquid alone or its combination with TOPO extractants. Both phases were mixed using thermostatic shaking water (conventional extraction, memmert model, WNB14) or ultrasonic bath, including an immersed probe system (sonicator 3000) adjusted to 24 W.

After a specific time, both phases were transferred into the decanter, and ICP-instrument analyzed the concentration of the aqueous phase.

3. Evaluation Parameter

The variations in the metal ion concentrations of two phases are the criteria for examining the extraction performance, which is determined by the distribution ratio (D), and the extraction efficiency (%E), separation factor (SF), and stripping percent (%S) according to the following equations:

$$D=\frac{[Dy^{3+}]_{org,\ after\ extraction}}{[Dy^{3+}]_{aq,\ after\ extraction}} \quad (1)$$

$$\%E=\frac{[D]}{[D]+\left(\frac{V_{aq}}{V_{org}}\right)}\times 100 \quad (2)$$

$$SF=\frac{D_{Dy}}{D_{Pr\ or\ Nd}};\ SF=\text{Separation factor} \quad (3)$$

$$\%S=\frac{[M^{3+}]_{in\ aqueous\ phase}}{[M^{3+}]_{in\ organic\ phase}}\times 100 \quad (4)$$

Dy (III) ions were recovered from the organic phase with nitric acid stripping solution by using Eq. (4) to determine the percentage of stripping.

4. Counter-current Extraction Procedure

The spent NdFeB magnet containing 23.4±0.1 Nd, 2.71±0.03 Pr, 0.98±0.01 Dy, 69.4±0.03 Fe, and 0.3±0.02 B was leached by 0.5 M HCl at 368 K and 100 g/L pulp density for 300 min. The obtained solution from the leaching process contained 16.73 g/L Nd, 3.66 g/L Pr and 0.34 g/L Dy along with only 0.012 g/L Fe and other minor impurities. Iron and other impurities were removed by precipitation at pH 3.5. The counter-current procedure was performed using separator funnels, in which 10 cm^3 of the aqueous phase and 10 cm^3 of the organic phase were introduced. The metal concentrations in the feed solution corresponded to the representative REE concentrations on magnet wastes. The selected organic phase with optimum concentration was used for the counter-current extraction procedure. The experimental work started with two separator funnels (funnel 1 and funnel 2) with A/O phase ratio equal 1 : 1. The steps described below were followed when both phases were separated: (1) Take a new separator funnel (number 2); a new organic phase is introduced in this funnel. (2) Remove the aqueous phase from the separator funnel number 2 as a sample. (3) Put raffinate from funnel number 1 into funnel number 2. (4) A fresh aqueous phase in the separator funnel number 2 is introduced. This procedure was repeated until the rare earth concentrations were constant. The stabilization was examined by determining rare earth concentrations in the stripping solution from the remaining organic phases.

5. Uncertainty Analysis by Using Monte Carlo Simulation

As perhaps the most extensively utilized technique for probabilistic risk assessment modeling, Monte Carlo simulation is a methodology that can assess the variability and uncertainty in several parameters. In the present investigation, the inconstancy and sensitivity examination of the predictions of the risk assessment model was completed utilizing Monte Carlo simulation. A streamlined way to deal with performing Monte Carlo simulation is to make the model without uncertainty in Microsoft Excel programming, then, at that point, utilize the spreadsheet-based application, for example, @Risk programming. The Monte Carlo simulation technique did the sensitivity analysis by 10,000 in @Risk 5.x. This technique chooses the upsides of the boundaries from their distribution fitted to include information and thus computes both point value and the distribution of exposure and risk. The risk investigation utilizing @Risk 5.x depends on fostering a mathematical model in Excel that represents the situation of interest. After developing a deterministic model, point estimates are replaced with probability distribution assumptions and forecast the output distribution. The determined output distribution is utilized to evaluate the riskiness of the situation.

The uncertainties because of the error in ion concentration analysis were assessed by utilizing a Monte Carlo technique. The actual measurement value was assumed to possess a Gaussian probability distribution with the mean and standard deviation corresponding to measured values and errors. Calculations randomly chose values to depend on the probability distribution for the various factors, and corresponding values for extraction efficiency evaluated in each run. A total of N=10,000 iterations were performed for each data point, and each simulation reran 100 times until the extraction efficiency value converged for the calculations. Due to uncertainty in essential variables, the propagated error was then calculated as the standard deviation of extraction efficiency values acquired over simulations.

RESULTS AND DISCUSSION

1. Effect of Time and Ultrasonic Waves

The extraction process was studied at different time intervals, which is shown in Fig. 1. After thirty minutes, the transfer of ions under mechanical mixing using a water shaker showed maximum efficiency for various solvents. The ultrasound-assisted extraction techniques described that maximum efficiency was achieved after fifteen minutes for the organic phase with pure ionic liquids or mixtures of ionic liquids with TOPO extractant. A comparison of results under ultrasonic conditions and mechanical mixing showed that ultrasonic waves led to a higher extraction efficiency in a shorter time. The sonication time of five minutes helps quickly provide

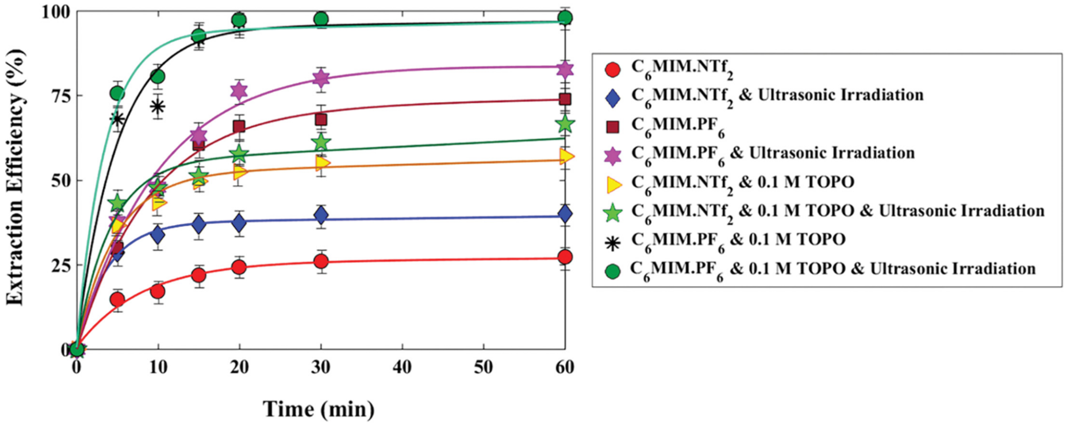

Fig. 1. Extraction Efficiency of Dy(III) versus time under mechanical and ultrasonic irradiation procedure ([Dy(III)]=250 ppm; pH=5; T=25 °C; O/A=1).

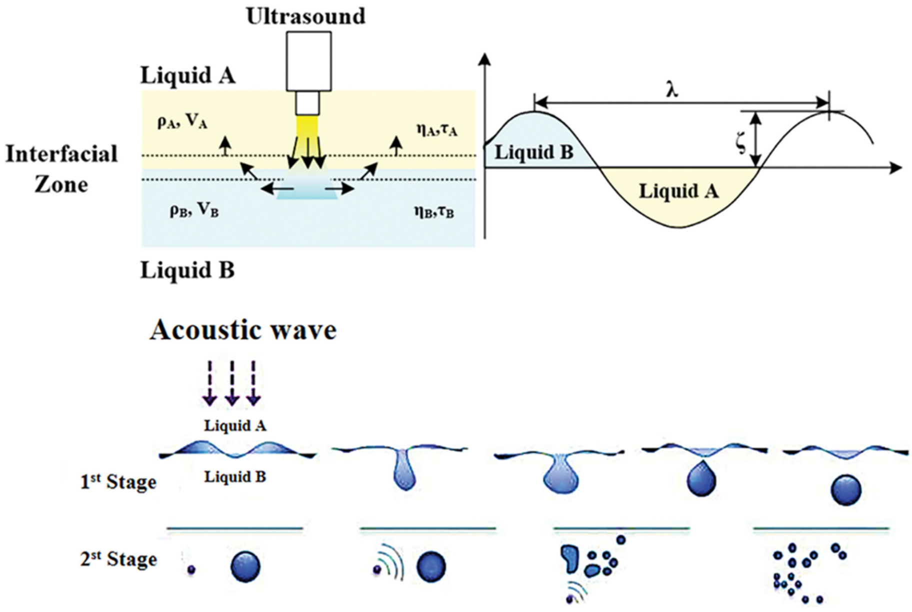

Fig. 2. Schematic illustration of emulsification by ultrasound and acoustic cavitation in the liquid-liquid interface [51].

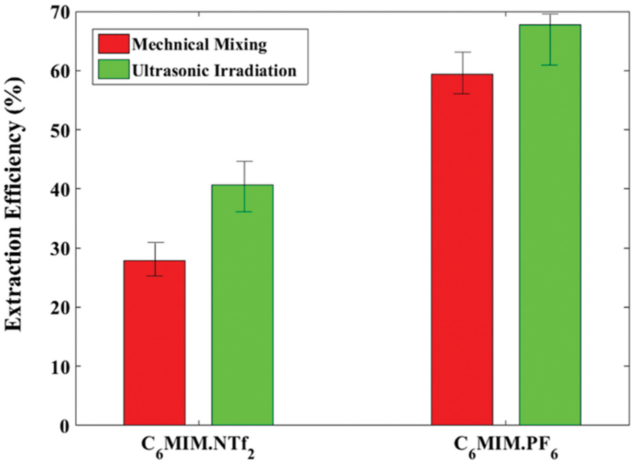

Fig. 3. Effect of pure ionic liquids for Dy(III) extraction ([Dy(III)]=250 ppm; pH=5; T=25 °C; O/A=1).

70% of the maximum efficiency by transferring Dy(III) ions to the organic phase. The increment in extraction efficiency indicated that the elimination of stagnant areas, more significant turbulence in the interface, and increased energy to the molecules are the reasons for modifying efficiency. The extraction process under ultrasonic conditions is shown in Fig. 2. The ultrasound propagates as a longitudinal wave of acoustic pressure with periodic rarefaction and compression cycles with a specific velocity distribution in an organic-aqueous phase interface. The interfacial area acts as an acoustic boundary with an acoustic impedance characteristic for each of the liquids. A specific cavitation threshold value causes acoustic emulsification, which involves initial droplet formation and breakup. The cavitation bubble implosion induces various collisions and enhanced diffusion of the extractable compounds into the organic phase. Therefore, more efficiency is achieved in the solvent extraction process under ultrasonic waves.

2. Effect of Ionic Liquids

The effects of ionic liquids on the extraction of dysprosium ions are shown in Fig. 3. The results show that pure ionic liquid could directly participate in removing rare-earth ions without the participation of another extractant. The percentage of dysprosium extraction was 27.86±0.31% and 59.38±0.12% with the ionic liquids $C_6MIM.NTf_2$ and $C_6MIM.PF_6$, respectively. This figure also shows that the ultrasonic waves help increase the percentage of transported ions by applying pure ionic liquids. Under ultrasonic conditions, the %E of Dy(III) increases to 40.67±0.42% and 67.78±0.17% for $C_6MIM.NTf_2$ and $C_6MIM.PF_6$ ionic liquids, respectively. The generated heat under ultrasonic conditions reduces the viscosity of ionic liquids; the formation of emulsion solution is accompanied by an increase in Dy(III) extraction efficiency.

Different cations and anions in aqueous solution were evaluated in the experiments to investigate the mechanism of Dy(III) extraction with pure ionic liquids. The results are shown in Fig. 4. The results show that potassium ions or chloride anions do not affect extraction efficiency. The positive trend in increasing $[C_6MIM]Cl$ and the negative trend in increasing KPF_6 and $KNTf_2$ salts indicate the anionic extraction mechanism.

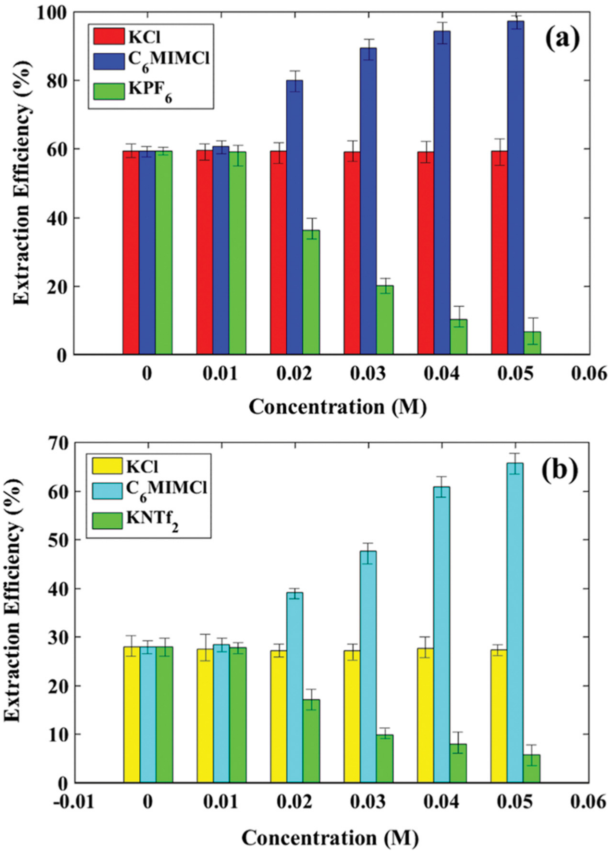

Fig. 4. Impact of initial concentration of $[C_6MIM]Cl$, KCl, KPF_6 and $KNTF_2$ on the extraction efficiency with (a) pure $C_6MIM.PF_6$ and (b) pure $C_6MIM.NTf_2$ ionic liquids ([Dy(III)]=250 ppm; pH=5; T=25 °C; O/A=1).

The diagram of the effect of various salt concentrations on the distribution ratio versus logarithmic form for both ionic liquids is shown in Fig. 5. According to this figure, two and one cations of C_6MIM^+ participate in the complex formation with Dy(III) ions for $C_6MIM.PF_6$ and $C_6MIM.NTf_2$ ionic liquids, respectively. The nitrate anions with a ratio of five and four parts for $C_6MIM.PF_6$ and $C_6MIM.NTf_2$ ionic liquids participate in complex formation. The PF_6^- and NTf_2^- showed the two and one parts with the reduction effect based on the reversed reactions. So, the reaction equations for complex formation could be described by the following equations:

$$2\overline{[C_6MIM]PF_6}+Dy^{3+}+5NO_3^- \leftrightarrow \overline{[C_6MIM]_2\cdot Dy(NO_3)_5}+2PF_6^- \quad (5)$$

$$\overline{[C_6MIM]NTf_2}+Dy^{3+}+4NO_3^- \leftrightarrow \overline{[C_6MIM]_2\cdot Dy(NO_3)_4}+NTf_2^- \quad (6)$$

A schematic of the process mechanism is shown in Fig. 6, and similar results have been reported in extraction with imidazole ionic liquids by Li and co-workers [44] and Wang and co-workers [45].

3. Effect of TOPO Extractant Concentration

The recovery of ions to the organic phase with 100% efficiency is a goal, which was investigated by examining the TOPO extractant effect and the mixture with ionic liquids. The outcomes appear in Fig. 7, and the presence of TOPO is associated with an increase in the Dy(III) extraction into the organic phase.

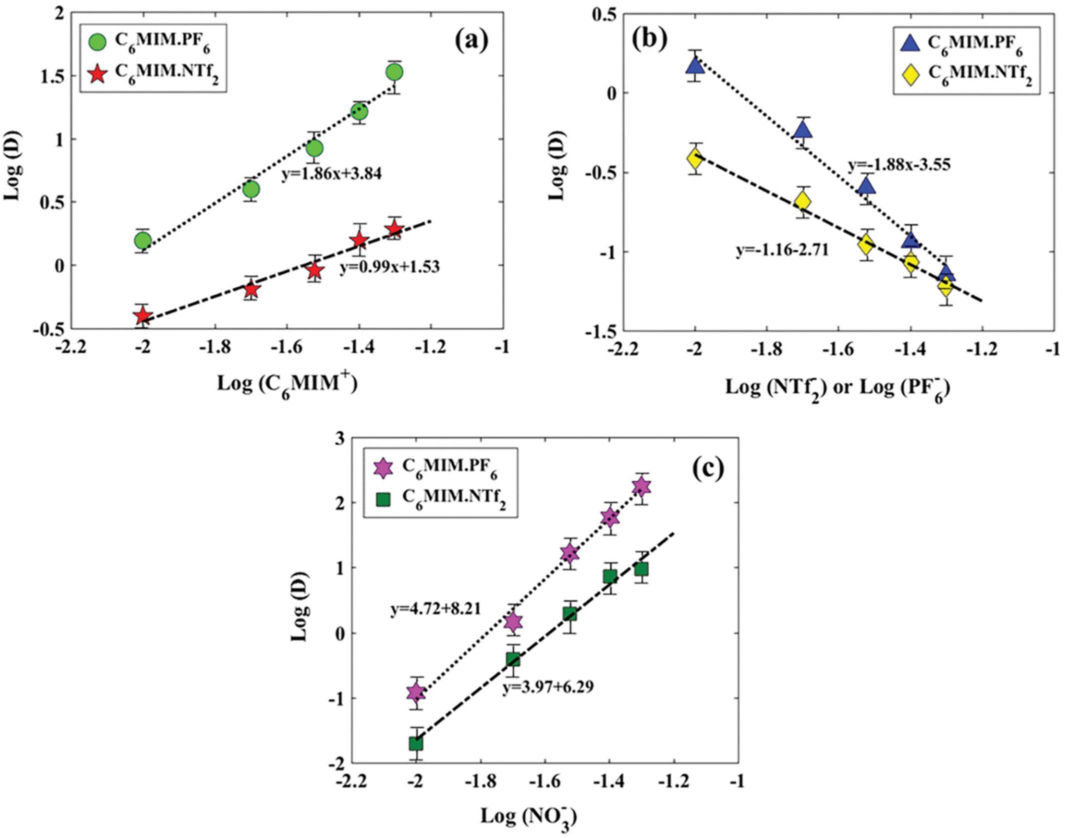

Fig. 5. Slope analysis of the extraction Dy(III) ions with both ionic liquids.

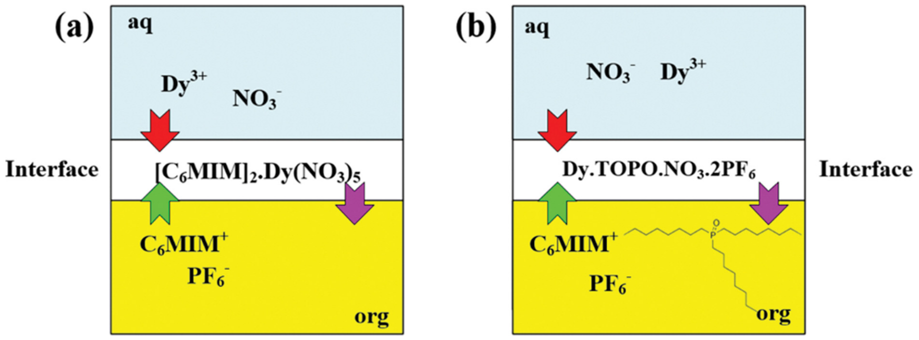

Fig. 6. Schematic of extraction mechanism with (a) pure ionic liquids and (b) mixture of TOPO extractant and ionic liquids for the extraction of dysprosium ions.

The synergistic effects of the extractant and ionic liquids are the reasons for the enhancement in extraction efficiency. The following equation can express the synergistic factor (R):

$$R=\frac{D_{1,2}}{D_1+D_2} \tag{7}$$

In the above equation, $D_{1,2}$ is the distribution ratio of a mixture of TOPO, and $C_6MIM.NTf_2$ or $C_6MIM.PF_6$. The coefficient of D_1 is related to the distribution ratio of TOPO extractant. Also, the D_2 is used for the distribution ratio of $C_6MIM.NTf_2$ or $C_6MIM.PF_6$. The results of the variation in the synergistic factor (R) are shown in Fig. 8.

This plot describes that the presence of extractants in the ionic liquid solvent is associated with the synergistic effect (R factor is higher than one). This value is effective in increasing the extraction of dysprosium ions from an aqueous solution. The effects of ultrasonic conditions are also visible in this diagram, which increases the extraction percentage. Creating more energy into the aqueous and organic phases causes an increase in the extraction efficiency of dysprosium ions.

The behavior of the traditional system containing kerosene and TOPO extractant for Dy(III) extraction is shown in Fig. 9. A comparison of this system with the ionic liquid system shows a higher %E with ionic liquids. It indicates that the ionic liquid system with

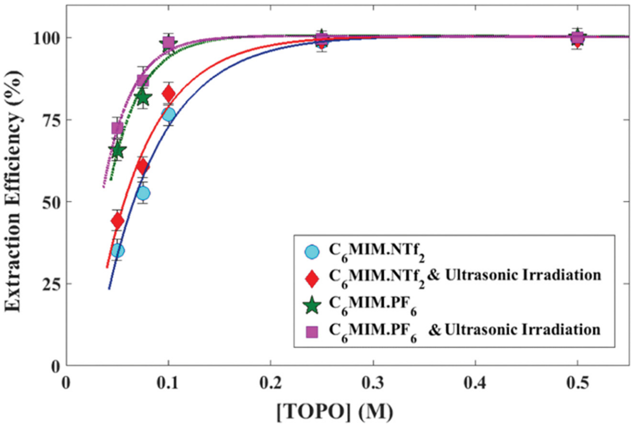

Fig. 7. Effect of mixture of ionic liquid with TOPO extractant for Dy(III) extraction ([Dy(III)]=250 ppm; pH=5; T=25 °C; O/A=1).

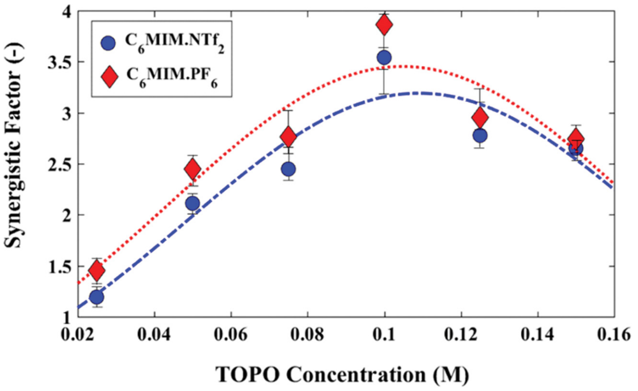

Fig. 8. Synergistic factor between ionic liquids and TOPO extractant.

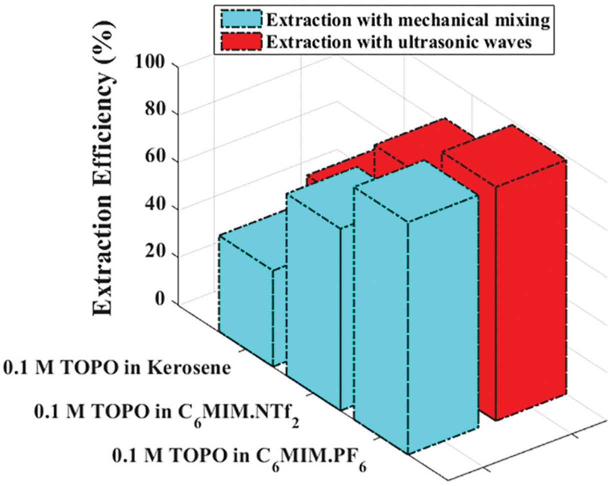

Fig. 9. Comparison of kerosene solvent and ionic liquids in the extraction of dysprosium ([Dy(III)]=250 ppm; pH=5; T=25 °C; O/A=1).

lower environmental impacts is more suitable for extracting rare earth elements. The ionic liquid acts as an extractant, and its pure form can be used to extract rare earth elements. Its combination with the trioctylphosphine oxide is associated with a synergistic effect, as shown in Fig. 8, which helps the increase in the extraction efficiency. But kerosene diluent is only used for a more straightforward dissolution of TOPO extractant and does not have synergistic effects. Therefore, the extraction rate is lower compared to the mixture of ionic liquid and TOPO extractant.

To describe the extraction mechanism of Dy(III) ions with TOPO in both ionic liquids and kerosene system, slope analysis was carried out as functions of equilibrium data from TOPO extractant concentration and nitrate ions in the aqueous phase.

According to Figs. 10(a) and 10(b), the equilibrium equation for Dy(III) extraction in kerosene system is presented by Eq. (8) as has been already reported [46].

$$Dy^{3+}+3\overline{TOPO}+3NO_3^- \leftrightarrow \overline{Dy\cdot 3TOPO\cdot 3NO_3} \tag{8}$$

In ionic liquids, it seems that more TOPO molecules are involved in the extraction reaction than the kerosene system. As shown in Figs. 10(a) and 10(b), the linear dependency with the slope of 5 was obtained for both ionic liquids. It indicates that five TOPO molecules coordinate to one metal ion in the extracted species in each system. The slope of linear dependency of Log D against nitrate concentration was one for both ionic liquid systems. A schematic of the extraction process mechanism is shown in Fig. 6, and the reaction equation can be expressed as follows:

$$\begin{aligned}&Dy^{3+}+4\overline{TOPO}+NO_3^-+2\overline{C_6MIM^+\cdot PF_6^-}\\&\Leftrightarrow \overline{Dy\cdot 4TOPO\cdot NO_3\cdot 2PF_6}+2C_6MIM^+\end{aligned} \tag{9}$$

$$\begin{aligned}&Dy^{3+}+4\overline{TOPO}+NO_3^-+2\overline{C_6MIM^+\cdot NTf_2^-}\\&\Leftrightarrow \overline{Dy\cdot 4TOPO\cdot NO_3\cdot 2NTf_6}+2C_6MIM^+\end{aligned} \tag{10}$$

Furthermore, the effect of the [C_6MIM^+] concertation in the aqueous phase on the extraction of Dy(III) with both ionic liquids was examined by adding C_6MIMCl to the aqueous phase as a source of [C_6MIM^+]. A reduction in Log(D) inversely with the concentration of this ion is shown in Fig. 10(c). This behavior supports the extraction mechanism expressed by Eqs. (9) and (10). The presence of TOPO extractant helps to reduce the tendency of dysprosium ions to form complexes with nitrate anions and to participate freely in the aqueous phase for complex formation.

Two ionic liquid systems are compatible with such "large ionic complexes" of dysprosium ions with TOPO extractant. It may be due to a characteristic of ionic liquids such as polarity and iconicity. However, this phenomenon did not appear in the ionic liquid mixture with other neutral extractants such as CMPO extractant [47]. Because the TOPO molecule is smaller and the structure is more straightforward than that of CMPO, which has two coordinate sites P=O and C=O whereas TOPO has only one site P=O.

4. Effect of Aqueous Phase Acidity

The acidity of the aqueous phase affects the transfer of ions between two phases, and its impacts are shown in Fig. 11. The results of the variation in this figure show that the pH parameter (>3) causes an increment in %E with the presence of TOPO extractant in the ionic liquid solvent. In pH<3, the protonation of neutral extractant increments and its contribution decreases for the reaction with Dy(III) ions. Further acidity causes a gradual increase in

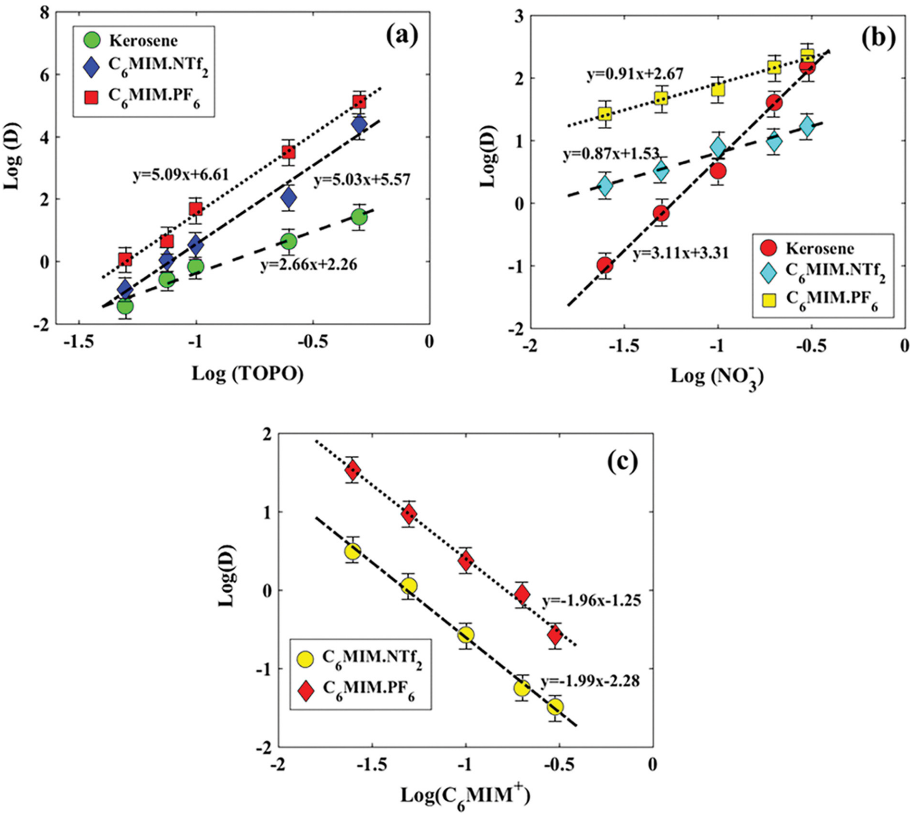

Fig. 10. Logarithmic value of distribution ratio versus (a) TOPO concentration, (b) NO_3^-, (c) C_6MIM^+ ([Dy(III)]=250 ppm; pH=5; T=25 °C; O/A=1).

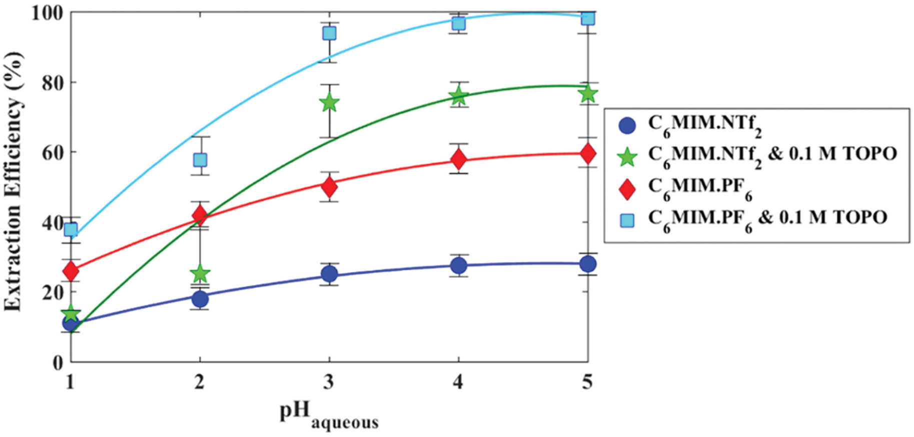

Fig. 11. Variation of extraction efficiency with aqueous phase acidity ([Dy(III)]=250 ppm; T=25 °C; O/A=1).

$[C_6MIM]^+$ ions in the aqueous solution. The decomposition of ionic liquids occurs due to ion exchange between PF_6^- and NO_3^- and acid-catalyzed hydrolysis of PF_6^- to PO_4^{3-}. The ionic liquid $C_6MIM.NTf_2$ is more stable, but its decomposition increases with increasing aqueous phase acidity and the replacement of NTf_2^- with nitrate ions.

In the free extraction medium of TOPO, the effects of acidity on the ionic solvent are low and slight increase is observed in the experiments. Increasing the values of $[C_6MIM]^+$, according to Fig. 4 and Eqs. (5) and (6), helps the increase in the extraction rate. Similar results have been reported by Chen et al. [48] and Li et al. [44].

5. Effect of Temperature

The study of temperature on the distribution ratio and extraction efficiency is illustrated in Table 1. The results demonstrate that the enhancement in the temperature shows a slight reduction in the extraction efficiency. Based on the van't Hoff equation, the enthalpy extraction process is obtained equal to −8.53±0.12 KJ/mol and −12.47±0.45 KJ/mol for [$C_6MIM.PF_6$ & 0.1 M TOPO] and [$C_6MIM.NTf_2$ & 0.1 M TOPO], respectively, with exothermic behavior.

Table 1. Effect of temperature on the distribution ratio and extraction efficiency for the mixture system of ionic liquids and TOPO extractant ([Dy(III)]=250 ppm; pH=5; O/A=1)

Temperature (°C)	C_6MIM.NTf$_2$ & 0.1 M TOPO		C_6MIM.PF$_6$ & 0.1 M TOPO	
	Distribution ratio (D)	Extraction percent (%)	Distribution ratio (D)	Extraction percent (%)
25	3.27±0.12	76.58±0.19	46.89±0.32	97.91±0.25
35	2.87±0.21	74.18±0.17	40.25±0.25	97.58±0.29
45	2.31±0.16	69.82±0.23	37.76±0.12	97.42±0.17
55	2.11±0.25	67.82±0.27	33.67±0.31	97.12±0.11

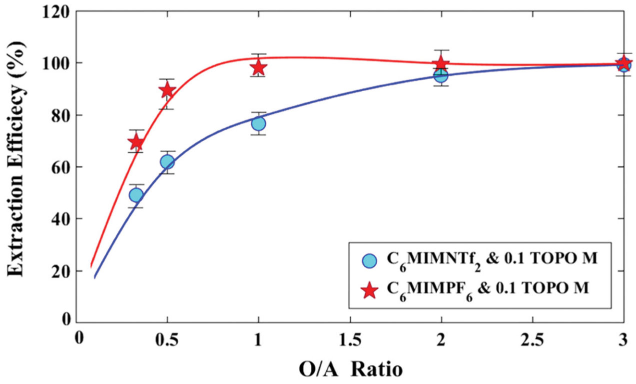

Fig. 12. Variation of extraction efficiency with organic/aqueous phase ratio ([Dy(III)]=250 ppm; pH=5; T=25 °C).

Increasing the temperature causes a reduction in viscosity, which helps to increase the extraction rate. However, the results of the exothermic behavior of the reaction indicate a decrease in the extraction with increasing temperature. So, the two effects are opposite each other, and the increasing temperature does not cause drastic changes in the amount of extraction.

6. Effect of O/A Ratio

In Fig. 12, the effect of the organic phase on aqueous solution is shown by examining the increment in the extraction phase. This figure shows that the increase in the organic phase and the presence of ionic liquid along with the TOPO extractant helps increase the extraction of dysprosium and higher transfer into the organic phase with more complexes in the surface between both phases. O/A ratios equal to 1 and 2 are optimal ratios for extraction with C_6MIM.PF$_6$ and C_6MIM.NTf$_2$.

7. Effect of Stripping Phase

The results of dysprosium recovery from the organic phase by examining different nitric acid concentrations are presented in Table 2. Stripping of Dy(III) ions with nitric acid at low concentrations (0.5 M) indicates that the recovery conditions at low concentrations are the extraction process's desirability.

8. Environmental Effects of Ionic Liquids

Comparisons of solvents and their environmental effects reveal that ionic liquid solvents are more suitable for extraction. Due to the formation of hydrolysis and production of HF with C_6MIM.PF$_6$, this ionic liquid could not be used in the category of green solvents. The $[PF_6]^-$ was observed to be chemically and thermally stable at moderate experimental conditions, although decomposition becomes significant under acidic conditions lower pH~3 or high temperatures (343 and 373 K) [49]. Therefore, the extraction conditions in this system show that a medium with low acidity and pH higher than 5 is suitable for extraction, which reduces the effects of solvent hydrolysis and its adverse environmental impacts are not apparent in the experiments. Another issue in choosing solvents is the cost and energy consumption to produce them. Ionic liquids are synthesized with much energy consumption and this can affect their selection. However, Ghorbani and Simone's studies reported that the imidazolium ionic liquids with high purity could be produced in conditions with low cost and commercially available starting materials [50].

9. Results of Uncertainty Analysis

Uncertainty can be portrayed as an absence of information concerning the actual value of a parameter. Since numerous parameters are compelling in making a risk assessment, determining the most influential parameter can be helpful for better extraction efficiency. So, in this research, sensitivity analysis was used to deter-

Table 2. Stripping percent of Dy(III) ions with various concentrations of nitric acid

HNO_3 (M)	Without ultrasonic waves		With ultrasonic waves	
	C_6MIM.NTf$_2$ & 0.1 TOPO	C_6MIM.PF$_6$ & 0.1 TOPO	C_6MIM.NTf$_2$ & 0.1 TOPO	C_6MIM.PF$_6$ & 0.1 TOPO
0.1	43.22±0.25	33.88±0.27	52.66±0.15	36.78±0.09
0.25	65.88±0.11	48.77±0.24	71.23±0.19	58.99±0.16
0.5	95.43±0.12	92.66±0.21	98.55±0.12	94.99±0.18
0.75	97.33±0.17	92.71±0.15	98.65±0.16	95.44±0.11
1	97.56±0.28	92.75±0.16	98.76±0.19	95.74±0.09
1.5	97.99±0.17	92.83±0.12	98.43±0.13	96.15±0.11
2	96.01±0.15	92.05±0.25	98.03±0.12	96.01±0.09

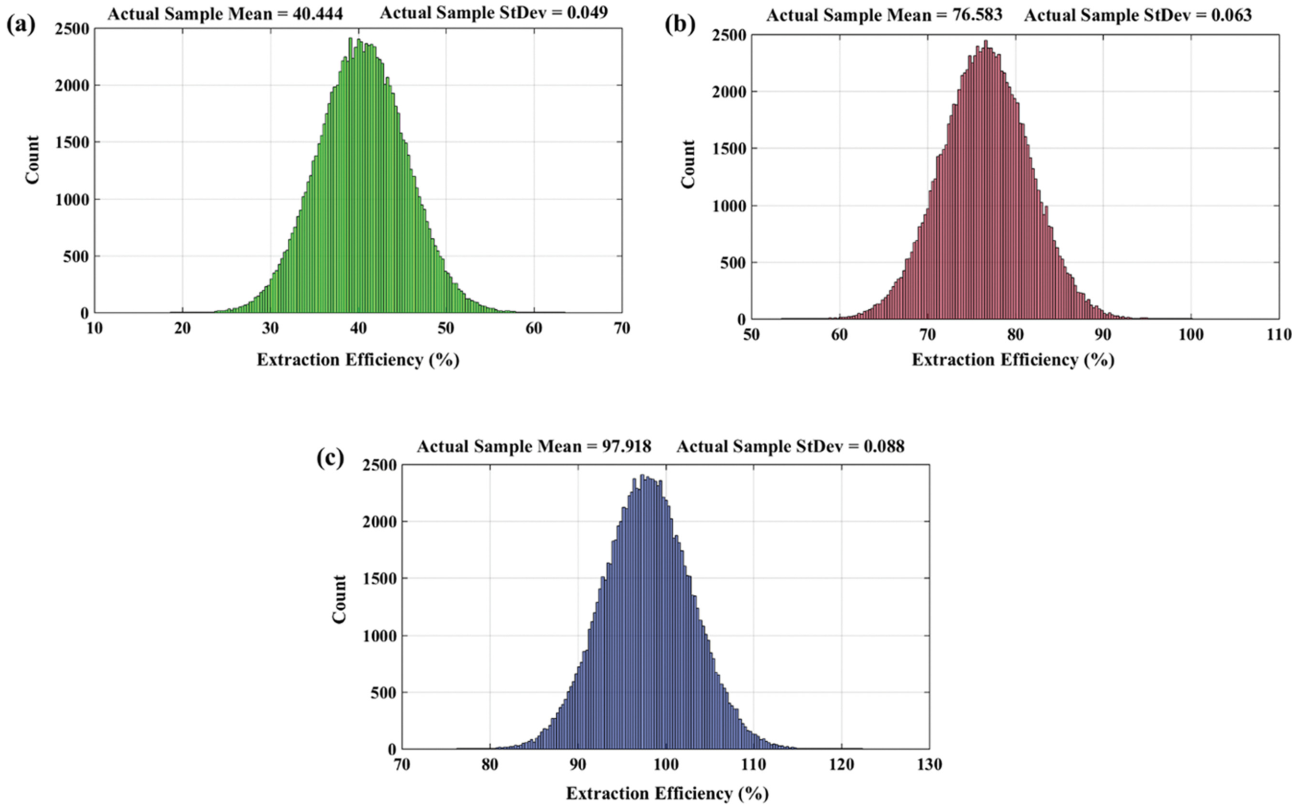

Fig. 13. Uncertainty analysis of extraction efficiency with mechanical mixing, (a) 0.1 M TOPO in kerosene, (b) 0.1 M TOPO in C_6MIM. NTf$_2$, (c) 0.1 M TOPO in C_6MIM.PF$_6$.

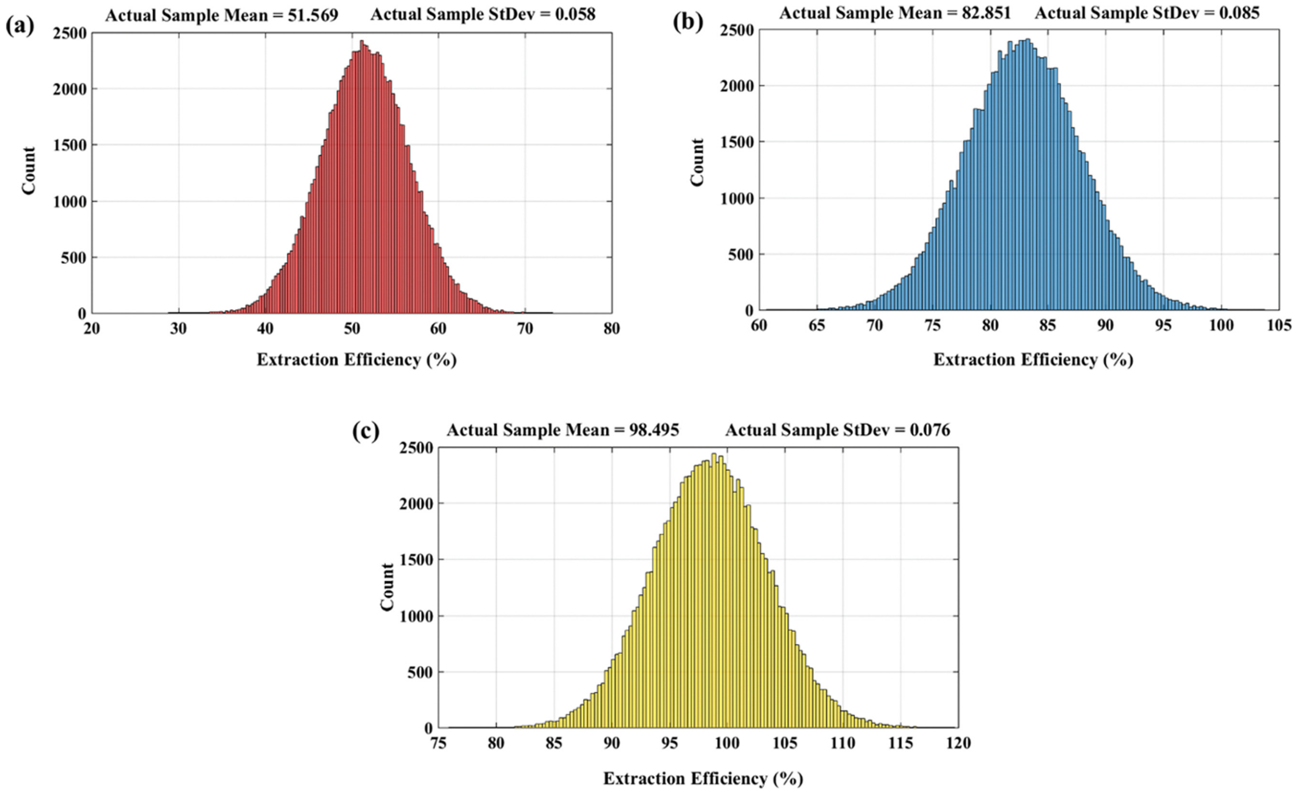

Fig. 14. Uncertainty analysis of extraction efficiency with ultrasonic waves, (a) 0.1 M TOPO in kerosene, (b) 0.1 M TOPO in C_6MIM. NTf$_2$, (c) 0.1 M TOPO in C_6MIM.PF$_6$.

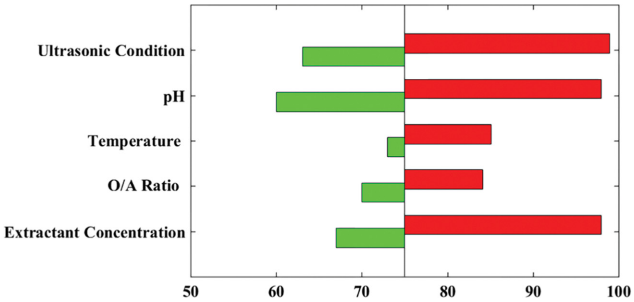

Fig. 15. Sensitivity analysis of the extraction efficiency.

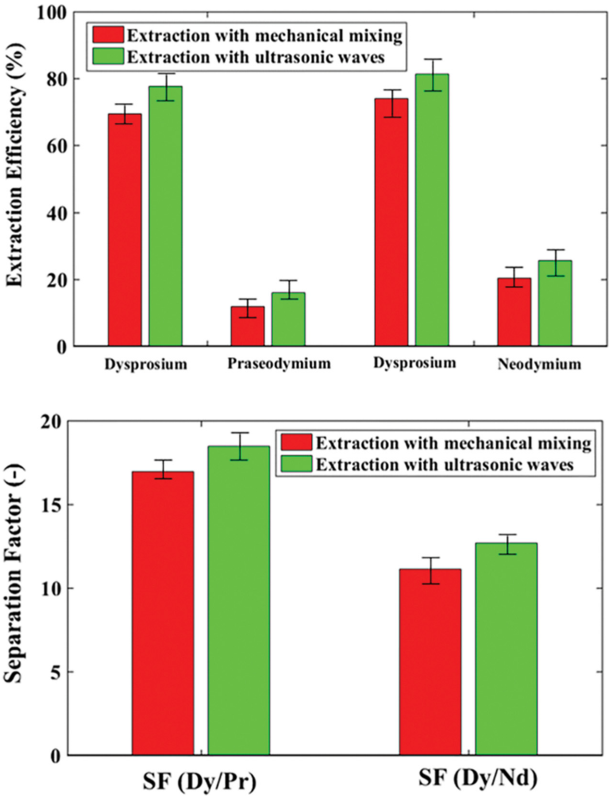

Fig. 16. Investigation of extraction efficiency and separation factor for binary system of ions with mixture of $C_6MIM.NTf_2$ ionic liquid and 0.1 M TOPO extractant ([Dy(III) or Pr(III) or Nd(III)]=250 ppm; pH=5; T=25 °C; O/A=1).

mine which variables and pathways most strongly influence the risk estimate. The effect of variables, including ultrasonic condition, pH, temperature, O/A ratio and extractant concentration, were selected to identify the most critical variables under uncertainty in the extraction efficiency. The contribution of parametric uncertainty analysis on the determination of the extraction efficiency was assessed using Monte Carlo simulation. A histogram of the probability distribution of the extraction efficiency is presented in Figs. 13 and 14. The results denote typical mean and standard deviation values used for variables with uncertainty.

The sensitivity analysis results are located on a bar diagram (Fig. 15), which shows the five major contributors to the uncertainty of the extraction efficiency. The sensitivity analysis of the model parameters indicated that the pH of the aqueous solution is the major source of uncertainty. The temperature parameter has the least sensitivity on the percent of extraction.

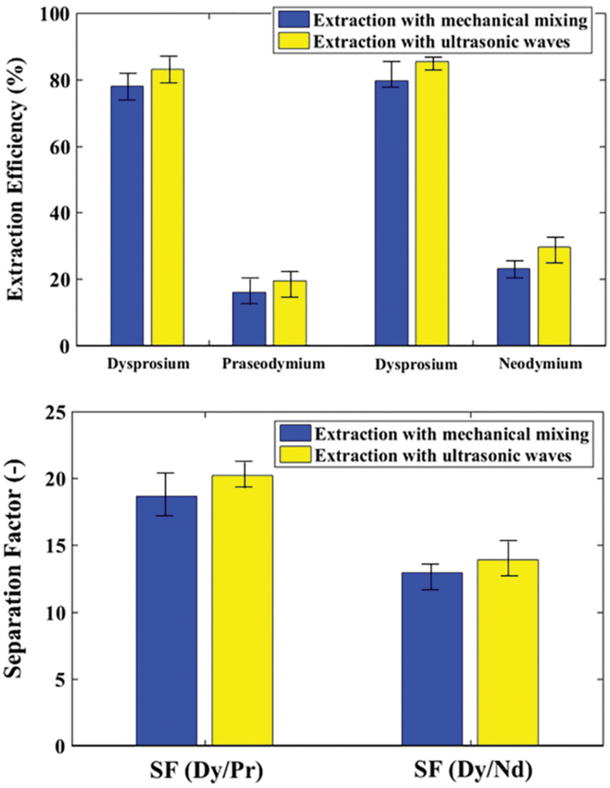

Fig. 17. Investigation of extraction efficiency and separation factor for binary system of ions with mixture of $C_6MIM.PF_6$ ionic liquid and 0.1 M TOPO extractant ([Dy(III) or Pr(III) or Nd(III)]=250 ppm; pH=5; T=25 °C; O/A=1).

10. Separation Factors with Binary Systems

The extraction of binary systems containing (Dy^{3+} and Nd^{3+}) or (Dy^{3+} and Pr^{3+}) with 250 ppm concentration was investigated by application of ionic liquids (0.1 M TOPO in $C_6MIM.NTf_2$ or $C_6MIM.PF_6$). Figs. 16 and 17 show that the extraction efficiency decreased with the presence of other rare-earth ions in solution due to the contribution of these ions for complex formation.

As shown in Fig. 16, the separation factor of Dy(III)/Pr(III), Dy(III)/Nd(III) with 0.1 M TOPO in $C_6MIM.NTf_2$ was equal to 16.97 ± 0.17 and 11.14 ± 0.25, respectively. But with 0.1 M TOPO in $C_6MIM.PF_6$, as described in Fig. 17, the values of 18.63 ± 0.27 and 12.95 ± 0.14 were obtained for $SF_{Dy/Pr}$ and $SF_{Dy/Nd}$, respectively. The results showed that $C_6MIM.PF_6$ is more successful in separating the dysprosium ions from praseodymium and neodymium ions than $C_6MIM.NTf_2$.

Changing the mechanical condition to an ultrasonic-assisted technique also causes an increase in separation factors. The separation factors have been increased to 18.47 ± 0.26, and 12.69 ± 0.31 for $SF_{Dy/Pr}$ and $SF_{Dy/Nd}$ with 0.1 M TOPO+$C_6MIM.NTf_2$ and 20.23 ± 0.11, 13.88 ± 0.41 with 0.1 M TOPO+$C_6MIM.PF_6$.

The result shows that the ultrasonic agent accelerates the reaction rate with the metal complex with more excellent selectivity.

Table 3. Separation factors for rare earth element with a mixture of TOPO and ionic liquid from the leaching solution

	With mechanical mixing		With ultrasonic wave	
Concentration TOPO/M	$SF_{Dy/Nd}$	$SF_{Dy/Pr}$	$SF_{Dy/Nd}$	$SF_{Dy/Pr}$
$C_6MIM.NTf_2$				
0.025	9.31±0.43	3.71±0.21	10.04±0.65	4.11±0.36
0.05	10.23±0.31	6.78±0.39	11.34±0.53	7.32±0.58
0.1	11.37±0.52	8.93±0.11	12.06±0.12	9.11±0.68
$C_6MIM.PF_6$				
0.025	10.43±0.32	5.91±0.39	11.45±0.18	6.72±0.53
0.05	11.22±0.52	7.83±0.21	12.65±0.32	8.43±0.45
0.1	12.43±0.44	10.04±0.32	12.87±0.67	11.01±0.67

Therefore, intensification of the extraction of dysprosium ions from waste neodymium magnet solution was obtained under ultrasonic irradiation, and 0.1 M TOPO diluted in $C_6MIM.PF_6$.

11. Separation Factors with Leaching Solution

The solvent extraction and separation of rare earth elements from this leaching solution was carried out by a mixture of TOPO extractant and ionic liquids ($C_6MIM.NTf_2$, and $C_6MIM.PF_6$) in a single-step procedure. The separation factors ($\beta_{Dy/Pr}$ and $\beta_{Dy/Nd}$) are shown in Table 3. The highest separation factors between Dy and the light REE were reached in 0.1 M TOPO in $C_6MIM.PF_6$ under ultrasonic condition. Concentration Dy was extracted selectively from other elements and the light REE. This can be explained because the ion exchange mechanism governs the extraction, where Dy substitutes for Nd in the organic phase.

12. Result of Counter-current Experiments

The counter-current process was carried out the separation of rare earth from the spent NdFeB magnet waste solution. The TOPO concentration was 0.1 M, and $C_6MIM.PF_6$ was used as the diluent in the organic phase with the working conditions at A : O ratio of 1 : 1. As shown in Fig. 18(a), the McCabe-Thiele plot indicates that one stage is required to obtain the total elimination of Dy(III) from the aqueous phase. The measured concentrations of Dy(III), Pr(III), and Nd(III) in each phase for every step of the separation process are shown in Fig. 18(b) with the working conditions at A : O ratio of 2 : 1. The Dy(III) concentration in the raffinate gradually decreases while Nd(III) concentration remains constant throughout the whole process. This is because the heavy rare earths are extracted by higher extraction efficiency over the light rare earths. Conversely, the dysprosium concentrations increase in the loaded organic solutions. Consequently, the main objective of using a mixture of $C_6MIM.PF_6$ ionic liquid and TOPO extractant has been demonstrated in the counter-current extraction experiment.

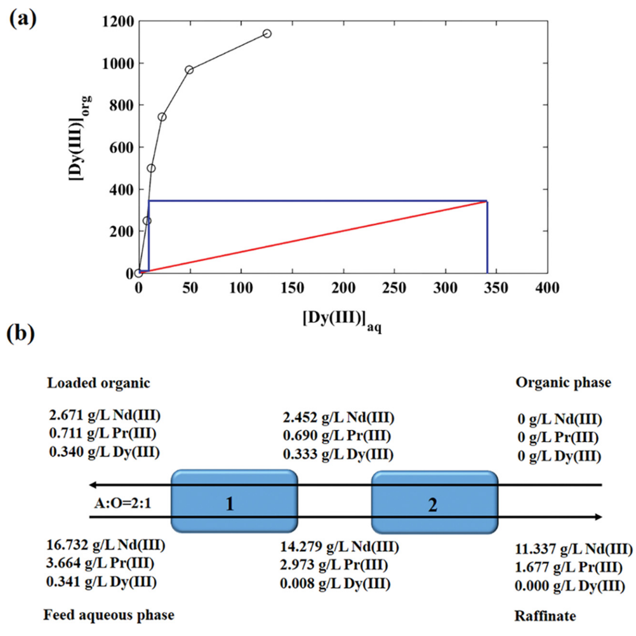

Fig. 18. (a) McCabe-Thiele plot for extraction of Dy(III) ions; (b) Counter-current extraction process with spent NdFeB magnet leaching solution.

CONCLUSION

This systematic experimental study with ionic liquids under ultrasonic waves was carried out for dysprosium ion extraction from an aqueous solution. The synergistic effect was investigated by mixing the ionic liquid and different concentrations of TOPO extractant. The results showed that the combination of ionic liquids with TOPO extractant increased extraction efficiency. This increase was higher for $C_6MIM.PF_6$ than for $C_6MIM.NTf_2$ ionic liquid. Better conditions with increasing ion transfer between two phases appeared in the extraction with ultrasonic waves compared to mechanical mixing. The results of effective parameters showed that ambient temperature, aqueous phase pH higher than three, O/A ratio equal to one, and the nitric acid concentration equal to 0.5 led to increased dysprosium extraction. Optimal conditions were provided for effective separation of dysprosium ions from neodymium and praseodymium ions from effluent neodymium magnet solution using trioctylphosphine oxide extractant (0.1 M) diluted in ionic liquid under ultrasonic conditions.

REFERENCES

1. D. A. Atwood, *The rare earth elements: Fundamentals and applications*, Wiley, New York (2012).
2. V. P. Menushenkov and A. G. Savchenko, *J. Magn. Magn. Mater.*, **272-276**, E1891 (2004).

3. S. Hirosawa, *JOM*, **67**, 1304 (2015).
4. M. Asadollahzadeh, R. Torkaman and M. Torab-Mostaedi, *Sep. Purif. Rev.*, **50**, 417 (2021).
5. J. Zhang, B. Zhao and B. Schreiner, *Separation hydrometallurgy of rare earth elements*, Springer, New York (2018).
6. M. K. Jha, A. Kumari, R. Panda, J. R. Kumar, K. Yoo and J. Y. Lee, *Hydrometallurgy*, **165**, 2 (2016).
7. B. K. Pramanik, L. D. Nghiem and F. I.Hai, *Water Res.*, **168**, 115149 (2020).
8. N. L. Nemerow, F. J. Agardy, F. Agardy and F. P. Agardy, *Strategies of industrial and hazardous waste management*, Wiley, New York (1998).
9. M. C. Bubalo, S. Vidović, I. R. Redovniković and S. Jokić, *J. Chem. Technol. Biotechnol.*, **90**, 1631 (2015).
10. B. Pospiech and W. Kujawski, *Rev. Chem. Eng.*, **31**, 179 (2015).
11. E. Rynkowska, K. Fatyeyeva and W. Kujawski, *Rev. Chem. Eng.*, **34**, 341 (2017).
12. M. J. Salar-García, V. M. Ortiz-Martínez, F. J. Hernández-Fernández, A. P. d. l. Ríos and J. Quesada-Medina, *J. Hazard. Mater.*, **321**, 484 (2017).
13. A. Ayati, S. Ranjbari, B. Tanhaei and M. Sillanpää, *J. Mol. Liq.*, **375**, 71 (2019).
14. M. Asadollahzadeh, R. Torkaman, M. Torab-Mostaedi, A. Ghaemi and A. Hemmati, *Int. J. Env. Anal. Chem.*, (2020). DOI:10.1080/03067319.2020.1789615.
15. M. Asadollahzadeh, R. Torkaman and M. Torab-Mostaedi, *Int. J. Env. Anal. Chem.*, (2020). DOI:10.1080/03067319. 2020.1763976.
16. M. Asadollahzadeh, R. Torkaman and M. Torab-Mostaedi, *Int. J. Env. Sci. Technol.*, **17**, 3983 (2020).
17. M. Asadollahzadeh, R. Torkaman, M. Torab-Mostaedi, A. Hemmati and A. Ghaemi, *Chem. Pap.*, **74**, 4193 (2020).
18. Y. Dong, X. Sun, Y. Wang, C. Huang and Z. Zhao, *ACS Sustainable Chem. Eng.*, **4**, 1573 (2016).
19. R. Turgis, G. Arrachart, V. Dubois, S. Dourdain, D. Virieux, S. Michel, S. Legeai, M. Lejeune, M. Draye and S. Pellet-Rostainga, *Dalton Trans.*, **45**, 1259 (2016).
20. H. Zhou, Y. Wang, X. Guo, Y. Dong, X. Su and X. Sun, *J. Mol. Liq.*, **254**, 414 (2018).
21. Y. Chen, H. Wang, Y. Pei and J. Wang, *Sep. Purif. Technol.*, **178**, 261 (2017).
22. S. Riañoa and K. Binnemans, *Green Chem.*, **17**, 2931 (2015).
23. L. Shen, J. Chen, L. Chen, C. Liu, D. Zhang, Y. Zhang, W. Su and Y. Deng, *Hydrometallurgy*, **161**, 152 (2016).
24. N. V. Thakur, *Solvent Ext. Ion Exc.*, **18**, 853 (2000).
25. E. Padhan and K. Sarangi, *Miner. Process Extrac. Met.*, **128**, 168 (2019).
26. N. E. El-Hefny, M. S. Gasser, S. Emam, W. H. Mahmoud, H. F. Aly, *J. Rare Earths*, **36**, 1342 (2018).
27. P. P. Sun, D.-H. Kim and S.-Y. Cho, *Miner. Eng.*, **118**, 9 (2018).
28. R. Torkaman, M. Asadollahzadeh and M. Torab-Mostaedi, *Chem. Eng. Process*, **111**, 7 (2017).
29. M. Asadollahzadeh, R. Torkaman and M. Torab-Mostaedi, *Geosystem Eng.*, **23**, 101 (2020).
30. M. Asadollahzadeh, R. Torkaman and M. Torab-Mostaedi, *Korean J. Chem. Eng.*, **37**, 322 (2020).
31. M. Asadollahzadeh, R. Torkaman and M. Torab-Mostaedi, *Sep. Seci. Technol.*, **56**, 1071 (2020).
32. M. Asadollahzadeh, R. Torkaman and M. Torab-Mostaedi, *ACS Omega*, **5**, 18700 (2020).
33. M. Asadollahzadeh, R. Torkaman, M. Torab-Mostaedi, A. Hemmati and A. Ghaemi, *Environ. Technol. Inno.*, **19**, 100979 (2020).
34. M. Asadollahzadeh, R. Torkaman, M. Torab-Mostaedi and F. Moazami, *Sep. Seci. Technol.*, **56**, 1241 (2019).
35. R. Torkaman, J. Safdari, M. Torab-Mostaedi, M. A. Moosavian and M. Asadollahzadeh, *J. Taiwan Inst. Chem. Eng.*, **48**, 18 (2015).
36. N. Ince, G. Tezcanli, R. Belen and İ. G. Apikyan, *Appl. Catal. B: Environ.*, **29**, 167 (2001).
37. J. Saien and S. Daneshamoz, *Ultrason. Sonochem.*, **40**, 11 (2018).
38. M. Daryabor, A. Ahmadi and H. Zilouei, *Ultrason. Sonochem.*, **34**, 931 (2017).
39. N. Stevanato and C. Silva, *Ind. Crop. Prod.*, **132**, 283 (2019).
40. R. Soltani, A. Shahvar, M. Dinari and M. Saraji, *Ultrason. Sonochem.*, **40**, 395 (2018).
41. T. Amiri-Yazani, R. Zare-Dorabei, M. Rabbani and A. Mollahossein, *Microchem. J.*, **146**, 498 (2019).
42. M. Behbahani, V. Zarezade, A. Veisi, F. Omidi and S. Bagheri, *Int. J. Env. Sci. Technol.*, **16**, 6431 (2019).
43. M. Sajid, M. K. Woźniak and J. Płotka-Wasylka, *Microchem. J.*, **144**, 117 (2019).
44. Y. Zuo, Y. Liu, J. Chen and D. Q. Li, *Ind. Eng. Chem. Res.*, **47**, 2349 (2008).
45. K. Wang, H. Adidharm, M. Radosz, P. Wan, X. Xu, C. K. Russell, H. Tian, M. Fan and J. Yu, *RSC Adv.*, **19**, 4460 (2017).
46. Y. A. El-Nadi, *Hydrometallurgy*, **119-120**, 23 (2012).
47. K. Nakashim, F. Kubota, T. Maruyam and M. Goto, *Ind. Eng. Chem. Res.*, **44**, 4368 (2005).
48. X. Sun, D. Wu, J. Chen and D. Li, *J. Chem. Technol. Biotechnol.*, **82**, 267 (2007).
49. M. G. Freire, C. M. S. S. Neves, I. M. Marrucho, J. o. A. P. Coutinho and A. M. Fernandes, *J. Phys. Chem. A*, **114**, 3744 (2010).
50. M. Ghorbani and M. I. Simone, *ACS Omega*, **5**, 12637 (2020).
51. D. Radziuk and H. Möhwald, *Phys. Chem. Chem. Phys.*, **18**, 21 (2016).